Biomechanical Evaluation of a Novel Anchorless Transosseous Suture

The Open-Box Technique in Rotator Cuff Repair

Zheng Yan,* MD (iD), Zhefeng Jin,* MD, Guoqing Cui,[†] MD, Liguo Zhu,* MD, Jie Yu,* MD, Yinzhe Cui,* MD, Minshan Feng,*[‡] MD, Jiawen Zhan,* MD, Guangwei Liu,*[‡] MS, Xiaohua Liu,* MD, Yan Li,* MD, and Jia Ma,*[§] MD (iD)
Investigation performed at Wangjing Hospital of China Academy of Chinese Medical Sciences, Beijing, China

Background: Some early biomechanical studies have pointed out that the strength of transosseous suturing is not quite satisfactory. Based on previous studies, we enhanced the strength-related factors and developed a high-strength transosseous suture method, open-box (OBOX), which may offer superior biomechanical strength.

Purpose/Hypothesis: The purpose of this study was to compare cyclic loading, ultimate load to failure, and failure mode of OBOX configuration with those of the anchorless X-box (XBOX) construct and the anchored double-row suture bridge (ADRSB) construct. It was hypothesized that the ultimate strength (US) of the OBOX configuration is similar to that of the ADRSB construct and higher than that of the XBOX construct.

Study Design: Controlled laboratory study.

Methods: A total of 24 fresh-frozen porcine cadaveric shoulders were randomized to 3 repair constructs (8 cases per group). The infraspinatus tendon was detached and repaired to the footprint of the supraspinatus with different repair constructs. Biomechanical testing involved initial preload, cyclic loading, and ultimate failure load. Cameras recorded the bare footprint area (BFA, %), optical markers monitored first-cycle excursion (FCE, mm), and cyclic elongation (CE, %). The US (N) was measured by a mechanical testing machine, and the failure mode was recorded.

Results: The mean US in the OBOX group (708.91 ± 116.34 N) was significantly higher than that in the XBOX group (466.58 ± 70 N) ($P < .001$) and similar to that in the ADRSB group (630.21 ± 106.52 N) ($P = .387$). CE significantly differed between XBOX and ADRSB ($P = .019$), but not between OBOX and XBOX, or between OBOX and ADRSB. The ADRSB group had better fatigue resistance than the OBOX group. In addition, there were no significant intergroup differences in FCE or BFA in the initial and final cycles. The order of the failure mode incidence was as follows: XBOX > OBOX = ADRSB for type 1 tendon tear, OBOX > XBOX = ADRSB for type 2 tendon tear, and ADRSB > OBOX = XBOX for fixing material-related failure.

Conclusion: The OBOX construct demonstrated significantly higher mean US than the XBOX construct in the porcine cadaveric model and was comparable with ADRSB repair. The most common failure modes were type 2 tendon tear for OBOX, type 1 tendon tear for XBOX, and fixing material-related failure for ADRSB.

Clinical Relevance: The OBOX configuration represents a novel transosseous repair method with high fixation strength comparable with the ADRSB construct and stronger than the XBOX construct. However, caution is necessary because of the potential for type 2 tendon tear associated with OBOX, which could complicate revision procedures.

Keywords: biomechanical study; double-row suture bridge; rotator cuff repair; transosseous repair

Rotator cuff injury is a prevalent condition characterized by shoulder pain and dysfunction, with a prevalence rate[7] ranging from 13% to 32%. The primary challenge in rotator cuff repair lies in achieving a stable, durable, and cost-effective interface for tendon-bone fixation. The
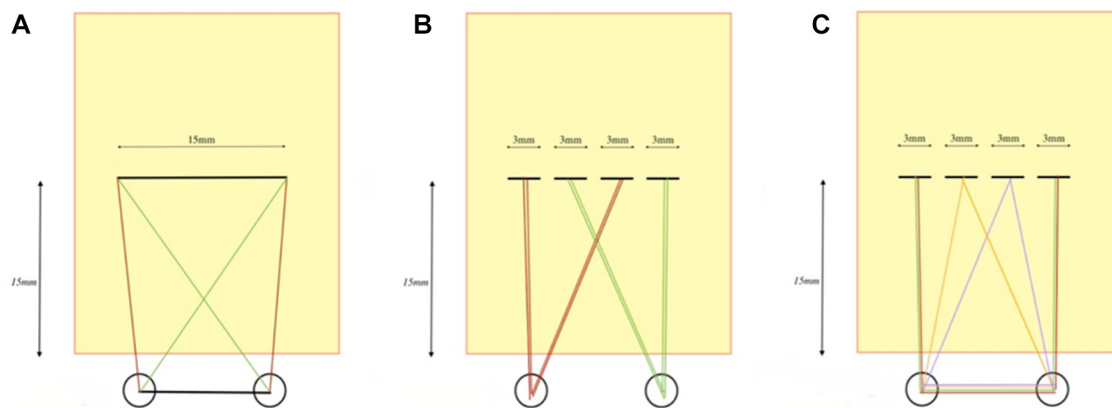
Figure 1. Three types of suture configuration. (A) XBOX. (B) ADRSB. (C) OBOX. ADRSB, anchored double-row suture bridge; OBOX, open box; XBOX, x box.

transosseous suture technique represents the gold standard in open surgical cuff repair. This cost-effective technique, with its advantages of promoting healing, minimizing anchor displacement, and facilitating repair in case of retear, has gained significant attention in recent years, particularly because of its applicability in arthroscopic procedures. Most studies[20] have reported favorable clinical efficacy and biomechanical properties, with the longest follow-up period spanning 10 to 18 years.

Several early biomechanical studies[18,23,31,37,38] reported suboptimal transosseous suture fixation strength. However, a recent meta-regression analysis reviewing 40 biomechanical studies has shown a limited association between construct strength and fixation type.[1] The type and number of sutures, suture limbs, and the inclusion of mattress stitches may serve as more reliable predictors of fixation strength compared with the type of construct. With the same number of suture limbs, there are no significant differences in biomechanical strength among single-row anchored, double-row anchored, transosseous equivalent, and transosseous repairs.[12] We developed a technique for transosseous repair using more sutures, suture limbs, and mattress stitches than the X-box (XBOX) configuration, called the open-box (OBOX) configuration.

The suture configuration of OBOX (Figure 1A) bears resemblance to that of the anchored double-row suture bridge (ADRSB) (Figure 1B) and encompasses additional factors associated with fixation strength, surpassing those offered by the XBOX technique (Figure 1C). This study

hypothesized that the biomechanical strength of the OBOX configuration is much higher than that of the traditional transosseous suture in the XBOX technique and is similar to that of the ADRSB technique. Consequently, we would be able to offer a viable high-strength transosseous suture method for clinical application.

METHODS

In this study, 24 fresh-frozen porcine cadaveric shoulders, with a mean age of approximately 12 ± 2 weeks, were utilized. The shoulders were randomly assigned to 1 of the 3 repair groups—OBOX, XBOX, and ADRSB. The randomization process was conducted using a random-number table, with the random-number generator in Microsoft Excel (Microsoft) employed for this purpose. There were no significant differences in the mean weight of the prepared specimens between the OBOX (655.86 ± 28.6 g), XBOX (639.94 ± 41.26 g), and ADRSB (626.51 ± 34.94 g) groups ($P = .272$). The time elapsed between the animal's death and freezing of the shoulder did not exceed 24 hours. Before the procedure, the specimens, which had been stored at $-22°C$, were thawed to room temperature. The dissection of all specimens and the subsequent orthopaedic surgery were performed by an experienced shoulder surgeon (J.M.) with the assistance of a senior surgeon (Z.J.). Specimens that exhibited damage to the infraspinatus

muscle or tendon, as well as any bone above the surgical neck of the humerus during specimen isolation or fabrication, were excluded from the study.

Specimen Preparation

All soft tissue around the humerus, except for the infraspinatus tendon and the muscle used for testing purposes, was meticulously removed, while a portion of the proximal scapula was retained for stable clamping. The selection of the infraspinatus muscle is based on previous studies[15,19] and the results of the pre-experiment of this study, considering its similarity to human anatomy in terms of tendon length and footprint. Moreover, the ultimate strength (US) result of the ADRSB construct in the pre-experiment of this study is 521 ± 36.6 N, which far exceeds the result of 175 ± 82 N from the repair to the original footprint of porcine infraspinatus in the literature,[11] and is closer to the US intervals of human shoulder joint specimens such as[12] 578.5 ± 123.8 N and[25] 558.4 ± 122.9 N. Subsequently, the infraspinatus muscle was carefully isolated and fully detached from its insertion on the greater tubercle of the humerus, simulating a complete avulsion of the rotator cuff tendon. To ensure secure positioning, the free lateral distal humerus was embedded in a polyvinyl chloride pipe using acrylic cement. Once the specimen met the necessary criteria, repair procedures were performed according to the randomized treatment group. All repair knots were tied using a standardized surgeon's knot technique, incorporating an additional 3 reversing half-hitches on alternating posts.

The experimental group (OBOX construct) was created using the following 7 steps: (1) Two sets of bone tunnels were made 15 mm apart in the greater tubercle adjacent to the cartilage margin using our self-designed special humeral guide for the transosseous suture method; (2) Six high-strength composite braided synthetic surgical No. 2 sutures (Delta Co) were introduced using a guideline. Sutures 1, 2, 3, and 4 were individually introduced into 1 of the bone tunnels, while sutures 5 and 6 were looped continuously through the 2 bone tunnels, with the guide line reserved at the suture button position; (3) The free infraspinatus tendon was marked 20 mm from the tearing edge, and the widest distance was measured as 15 mm from the tendon center. Eight suture limbs (5a, 6a, 1a, 2a, 3a, 4a, 5b, and 6b) were evenly passed through the tendon separately; (4) Suture limbs 1a and 2a, as well as 3a and 4a, were knotted together pairwise and pulled tightly in reverse. Then, suture limbs 1b and 3b, as well as 2b and 4b, were pulled in reverse through the 2 bone tunnels, after which each pair was individually knotted at the lateral ends of these tunnels; (5) Sutures 5a and 6a, as well as 5b and 6b, were knotted separately; (6) The guideline at the suture button position passed the 2 suture limbs (5a and 5b) across the suture button. Subsequently, sutures 5a and 6a, as well as sutures 5b and 6b, were knotted; and (7) Sutures 1a and 1b, 2a and 2b, 3a and 3b, and 4a and 4b, were knotted in a crossed X pattern, resulting in an OBOX construct with a "square" shape outside and a "X" shape inside, resembling a box that opens from the top (Figure 2).

The control group 1 (XBOX construct) was created as follows: (1) Using our specially designed humeral guide for the transosseous suture method, 2 sets of bone tunnels were made in the greater tubercle adjacent to the cartilage margin, with a separation of 15 mm; (2) Each set of bone tunnels was threaded with 3 high-strength composite braided synthetic surgical No. 2 sutures (Delta Co), guided by a guide line. The posterior bone tunnel accommodated sutures 1 to 3, while the anterior bone tunnel accommodated sutures 4 to 6; (3) A segment of the free infraspinatus tendon, measuring 20 mm from the tear edge, was selected. Two sutures were passed through the tendon at a central location with a separation of 15 mm, corresponding to the respective sutures from the 2 tunnel sites—sutures 1 to 3 from 1 site, and sutures 4 to 6 from the other site; and (4) Knots were tied separately for sutures 1a and 1b, and 6a and 6b. Knots 2a and 5b and 2b and 5a were tied in a crossed X-shape configuration, and knots 3a and 4a, and 3b and 4b were tied in a mattress square configuration. The sutures were securely fastened, resulting in an XBOX construct with an "X" shape within the peripheral "square" (Figure 3).

The control group 2 (ADRSB construct) was implemented as follows: (1) Two double-loaded 5-mm titanium anchors with No. 2 high-strength composite braided synthetic surgical sutures (SA-I; Delta Co) were inserted into the greater tubercle adjacent to the cartilage margin, spaced 15 mm apart; (2) The free infraspinatus tendon was identified at a distance of 20 mm from the tear edge. Eight suture limbs from 4 sutures (1a, 1b, 2a, 2b, 3a, 3b, 4a, and 4b) were threaded evenly from the 8 stitches; (3) Knots were tied at suture limbs 1a and 1b, 2a and 2b, 3a and 3b, and 4a and 4b; and (4) Two double-loaded 5-mm titanium anchors (SA-I; Delta Co) were placed as the lateral-row anchor sites in the lateral humeral cortex, positioned 10 mm below the lateral edge of the greater tubercle and in the same coronal plane as the 2 previously mentioned medial-row anchors. Suture limbs 1a and 5a, 1b and 5b, 4a and 8a, 4b and 8b, 2a and 7a, 2b and 7b, 3a and 6a, and 3b and 6b were knotted, and the final suture ends were secured in the ADRSB construct (Figure 4).

Biomechanical Testing

The humerus was immobilized using acrylic cement encapsulation and securely clamped with a specialized fixture on the suspension arm of a mechanical testing machine (Gerhon Corporation). The humerus was positioned at a 30° abduction angle. We simulated the anatomic positioning of the supraspinatus with the arm in 60° of abduction. According to Poppen and Walker,[21] this position produces peak muscle forces during elevation of the normal shoulder. We kept the humeral rotation neutral for all specimens, using the bicipital groove and lesser tuberosity as rotational landmarks. In addition, a special clamping was used to fix the proximal infraspinatus muscle and scapula connected to it, which was located approximately 10 cm
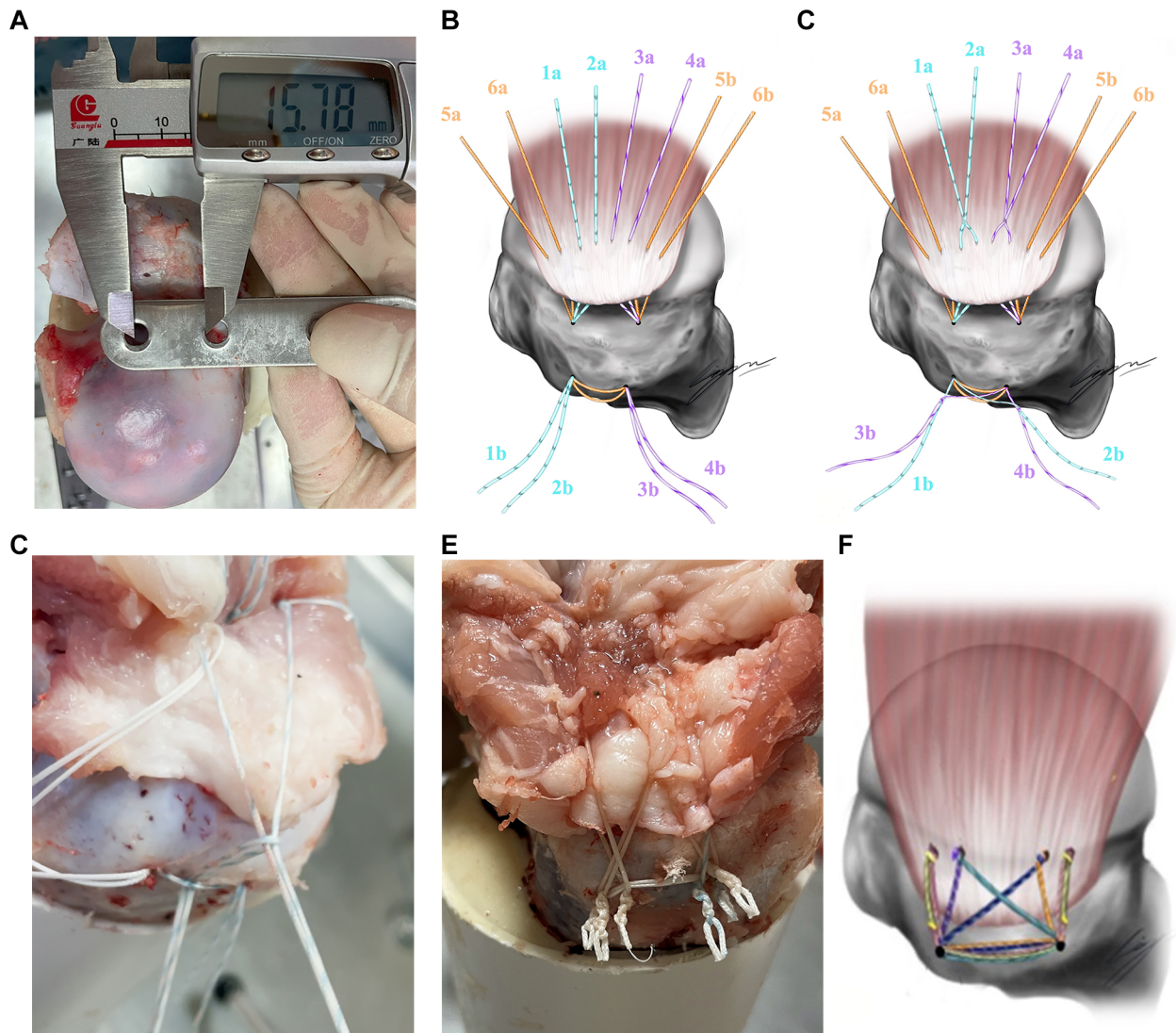
Figure 2. The experimental group (OBOX construct). (A) Vernier calipers were used to ensure a tunnel spacing of 15 mm. (B) Sutures were evenly passed through the tendon. (C) Sutures 1a and 2a, as well as 3a and 4a, were knotted together pairwise, and sutures 1b and 3b, as well as 2b and 4b, were pulled in opposite directions and knotted at the outer entrance of the tunnel. (D) A guide wire was placed for sutures 5a and 5b and guided across the suture button. After the 2 ends of the sutures 5 and 6, respectively, crossed the suture button, sutures 5a and 6a were tied together, and sutures 5b and 6b were also tied together. (E) The suture effect is shown in the gross specimen (porcine shoulder joint). (F) The schematic diagram shows the OBOX construct with a lateral ''square'' and a medial ''X'' shape with an opening on the top. OBOX, open box.

away from the tear edge, and positioned it at the lower end of the testing machine (Figure 5). The load was increased through the suspension arm of the testing machine.

The first-cycle excursion (FCE, mm) and cyclic elongation (CE, %) were monitored and assessed with 2 rows of reflective markers uniformly placed on the tendon surface. The lateral row consisted of 2 markers with 6 mm diameters (half-spheres fixed on thumbtacks) inserted into the bone just lateral to the repair site. The medial row consisted of two 6 mm–diameter markers pinned into the tendon, adjacent to the medial-row knots. Tracking the motion of the markers was accomplished using the OptiTrack

motion capture system (Version 1.10.1; Natural Point, Inc). The system employed a digital motion-capture lens, which provided precise measurements with an accuracy of 0.1 mm, capturing the x, y, and z coordinates in 3 dimensions.

Furthermore, the bursal side of the tendon was delineated by injecting methylene blue, specifically marking the projected edge of the tubercle covered by the repaired tendon. Throughout the experiment, a high-definition camera was employed to capture images at the preloaded state of 10 N, as well as at 180 N during the first and 100th cycles. These images were subsequently used to measure
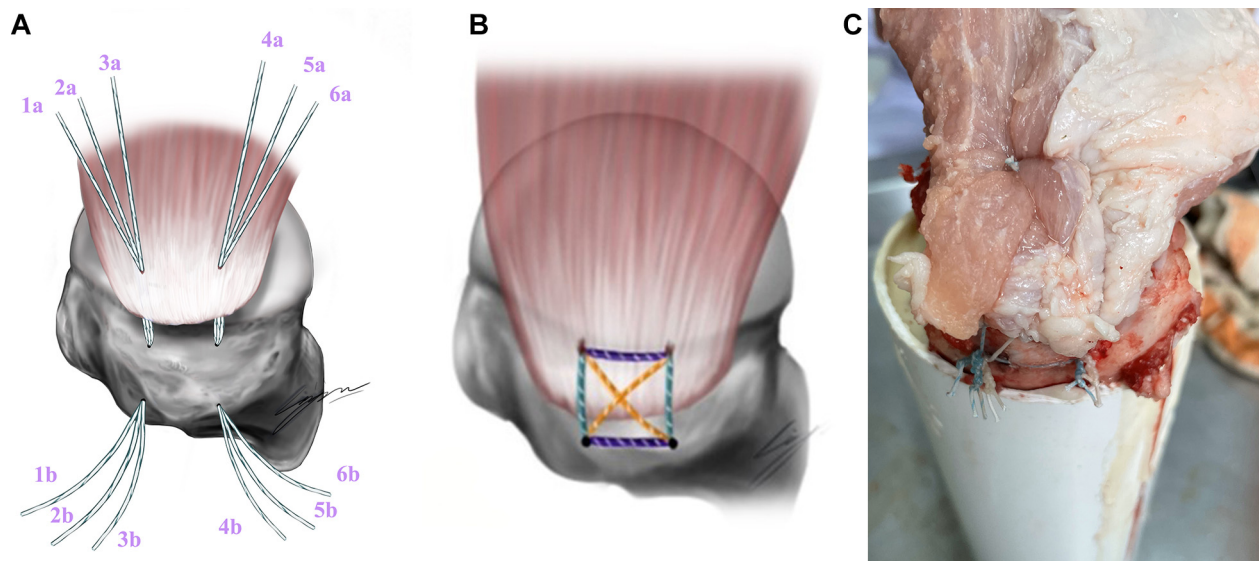
Figure 3. Control group 1 (XBOX construct): (A) Six X-box sutures were placed in 2 locations through the tendon. (B) Sutures 1a and 1b, as well as 6a and 6b, were knotted separately (green line); sutures 2a and 5b, as well as 2b and 5a, were knotted in a crossed X pattern (yellow line); and sutures 3a and 4a, as well as 3b and 4b, were knotted in a mattress pattern (purple line). The suture structure forms an XBOX construct with an ''X'' shape inside the peripheral ''square.'' (C) The X-box suture effect.
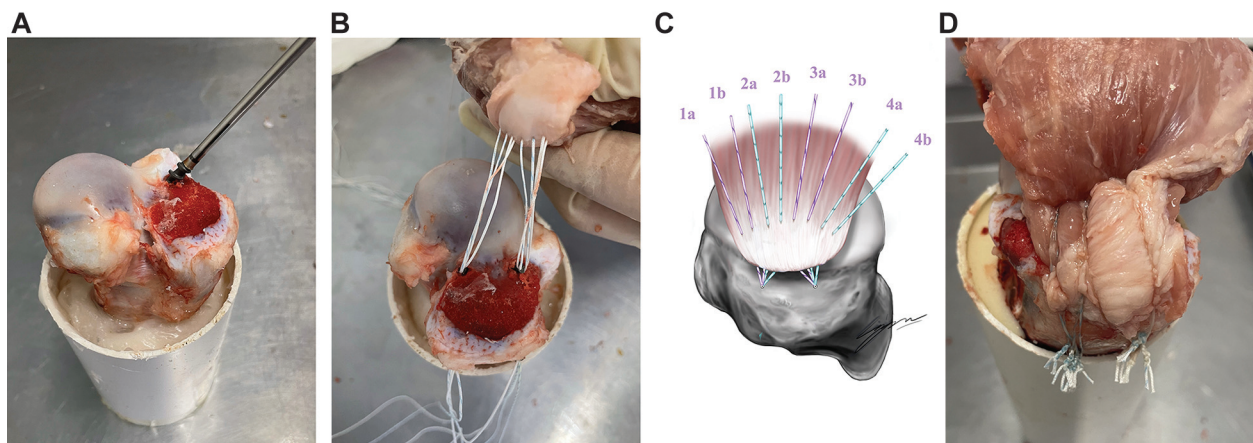

Figure 4. Control group 2 (ADRSB construct). (A) Medial row anchors were placed. (B) Sutures were placed evenly through the tendon. (C) Knots were tied between 1a and 1b, 2b and 2b, 3a and 3b, and 4a and 4b. (D) Suture effect on the gross specimen (porcine shoulder joint).

the loss of footprint coverage, identifying the bare footprint area (BFA, %).

To stabilize the specimen in the experimental setup, a 2-minute preload of 10 N in tension was applied to the repaired infraspinatus tendon. Fatigue resistance experiments were subsequently conducted, employing cyclic loads ranging from 10 to 180 N at a rate of 1 mm/s for a total of 100 cycles. The displacement tension curve graph illustrating these experiments is presented in Figure 6. If the preceding fatigue resistance experiments did not result in suture structure failure, the tendon was gradually retracted at a rate of 10 mm/s until complete rupture occurred. Failure strength was recorded at the moment

of failure. After the conclusion of the failure test, the condition of both the tendon and bone was meticulously documented, and encompassed the following: type 1 tear: failure at the site of repair, often with tendon detachment from the bone; type 2 tear: failure medial to the repair (muscle-tendon junction), with remnants of the tendon still attached to the bone; and fixing material-related failure of anchor or suture, which has not yet been formally defined in the literature.

The MATLAB software (MathWorks Inc) was utilized for optical data analysis, employing the 3-dimensional Euclidean space algorithm to calculate the mean medial-to-lateral distance between the 2 rows of marker points.
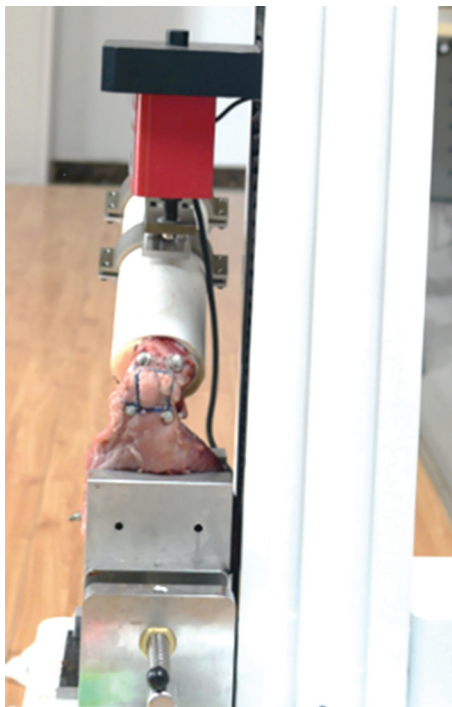
Figure 5. Special clamps for holding specimens in the mechanical testing machine.
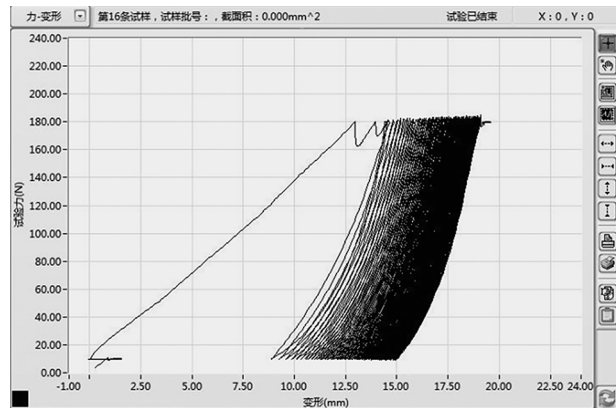

Figure 6. Typical progression during cycling testing. The horizontal axis represents the gap excursion, and the vertical axis represents the axial load of the traction machine.

The FCE was defined as the elongation of the construct from the preloaded state to the peak of the first cycle and was used to measure the initial stability of the construct. We determined the CE as a percentage of gapping from the preloaded state to the end of cyclic testing as follows: (Lf − Li)/Lp. Here, Li represents the mean distance between the 2 sets of marker points at the peak of the initial 5 cycles after the preloaded state, Lf represents the mean distance between the 2 sets of marker points at the peak of the final 5 cycles, and Lp represents the mean
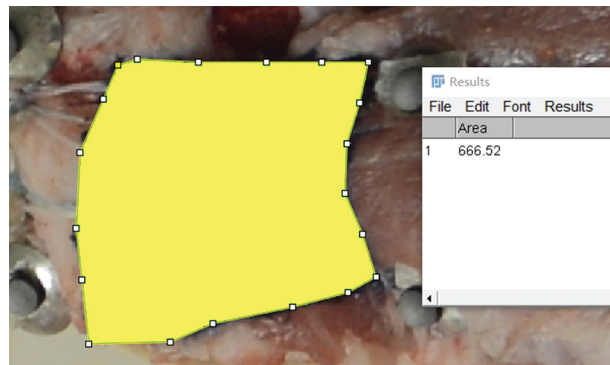

Figure 7. Measurement of the blank region's area using ImageJ 1.53 software.

distance between the 2 sets of marker points after the 10 N preloaded state.

The percentage of footprint coverage loss represents the portion of the total footprint exposed after each cyclic load. To analyze the BFA, ImageJ 1.53 software (National Institutes of Health) was employed to measure the area of the blank region within the methylene blue–marked area (Figure 7). Subsequently, the ratio of BFA from the initial cycle (Si) to the final 100th cycle (Sf) was calculated using Microsoft Excel 2021 (Microsoft). Specifically, the area of the blank region within the methylene blue-marked area when the tendon was subjected to a preload of 10 N was denoted as Sp. The ratio of the exposed area of the footprint area for the first cycle (BFA-Si) was calculated as (Si − Sp)/Sp, while the ratio of the exposed area of the footprint area at the end of the cycle (BFA-Sf) was calculated as (Sf − Sp)/Sp. If the value exceeded 100%, it was adjusted to 100% for statistical analysis.

The CE and BFA-Sf represented the endurance, and the FCE and BFA-Si indicated the initial stability of the structure. In the case of suture structure failure during loading, the US at the time of failure and the type of tear were recorded. The US was defined as the maximum force resisted by the construct.

Statistical Analysis

Statistical analysis was conducted using SPSS 26.0 software. Measurement data were presented as the mean ± standard deviation. For data that followed a normal distribution and exhibited homogeneity of variance, analysis of variance was employed, followed by post-hoc tests utilizing the Bonferroni method to determine significant differences. In cases where the measurement data did not conform to a normal distribution, the Kruskal-Wallis H test was utilized for comparisons. Count data were presented as the number of cases/percentages, and the χ^2 and Fisher exact probability tests were employed for comparisons. Post hoc tests for count data were conducted using the chi-square distribution (Bonferroni method). Statistical significance was defined as $P < .05$.

TABLE 1
Biomechanical Performance After Rotator Cuff Tear Repair[a]

Variable	ADRSB (n = 8)	OBOX (n = 8)	XBOX (n = 8)	F/χ^2	P
Cyclic elongation, %	3.83 ± 2.33	5.26 ± 3.04	7.19 ± 2.28	7.595	.022[b]
First-cycle excursion, mm	2.59 ± 1.19	2.59 ± 1.22	3.19 ± 1.9	0.44	.65
Ultimate strength, N	630.21 ± 106.52[b]	708.91 ± 116.34[b]	466.58 ± 70[a]	12.315	<.001[c]
BFA-Si, %	3.88 ± 1.44	4.67 ± 1.89	5.29 ± 1.73	1.378	.274
BFA-Sf, %	8.59 ± 1.49	8.07 ± 1.92	9.19 ± 2.33	0.656	.529
Tear mode				23.409	<.001[c]
T1	0 (0)	0 (0)	6 (75)		
T2	2 (25)	8 (100)	2 (25)		
F	6 (75)	0 (0)	0 (0)		

[a]Values are presented as mean ± SD. Cyclic elongation was assessed using the Kruskal-Wallis *H* test. First-cycle excursion, ultimate strength, BFA-Si, and BFA-Sf were assessed using ANOVA. The tear mode was assessed using the Fisher exact-probability test. The Bonferroni method was used for post-hoc tests: a < b. ADRSB, anchored double-row suture bridge construct; ANOVA, analysis of variance; BFA-Sf, footprint area at the end of the cycle; BFA-Si, ratio of the exposed area of the footprint area for the first cycle; F, fixing material-related failure; OBOX, anchorless open-box construct; T1, type 1 tear; T2, type 2 tear; XBOX, anchorless X-box construct.
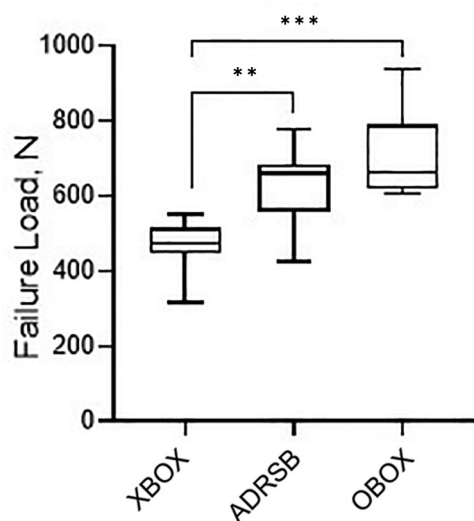[b]$P < .05$.
[c]$P < .01$.

Figure 8. Results of failure strength test (porcine specimens). ADRSB, anchored double-row suture bridge construct; OBOX, anchorless open-box construct; XBOX, anchorless X-box construct. **$P < .01$; ***$P < .001$.

RESULTS

In the failure test, the mean US of the OBOX group was significantly higher than that of the XBOX group ($P < .001$) and similar to that of the ADRSB group ($P = .387$) (Table 1 and Figure 8). The failure modes are summarized in Table 1. Therefore, the incidence of type 2 tendon tear was higher in the OBOX group than in the XBOX and ADRSB groups. Meanwhile, the XBOX mainly failed with type 1 tendon tear. In addition, fixing material-related failure was higher in the ADRSB group than in the OBOX and XBOX groups.

In cyclic testing, the difference in CE between the XBOX and ADRSB groups was statistically significant ($P = .019$), and the XBOX group had higher cyclic elongation. Nonetheless, no significant differences were observed between the OBOX and XBOX groups. No differences were found in CE and FCE between the ADRSB and OBOX groups. No significant intergroup differences were observed in the BFA-Si and BFA-Sf (Figure 9).

DISCUSSION

In this biomechanical analysis, the OBOX construct exhibited a significantly higher failure strength (708.91 ± 116.34 N) than the XBOX construct (466.58 ± 70 N) ($P < .001$), but similar failure strength to the ADRSB construct (630.21 ± 106.52 N). The CE and BFA-Sf were used as measures of the tendon's fatigue endurance under cyclic load. The CE showed no significant difference between the OBOX and ADRSB or XBOX constructs, while the ADRSB construct differed significantly from the XBOX construct ($P = .019$). However, there were no significant differences in BFA-Sf among the 3 constructs. The FCE and BFA-Si represented the initial stability of the constructs, and no significant differences were found in either of these parameters among the 3 structures. Optical data analysis revealed a significant difference in CE between the XBOX and ADRSB constructs, but there was no significant difference in BFA-Sf. Overall, the OBOX construct exhibited higher US and fatigue endurance compared with the XBOX construct, and its performance was comparable with that of the ADRSB construct.

Several clinical studies have confirmed the efficacy of the transosseous suture technique.[§] Some studies have

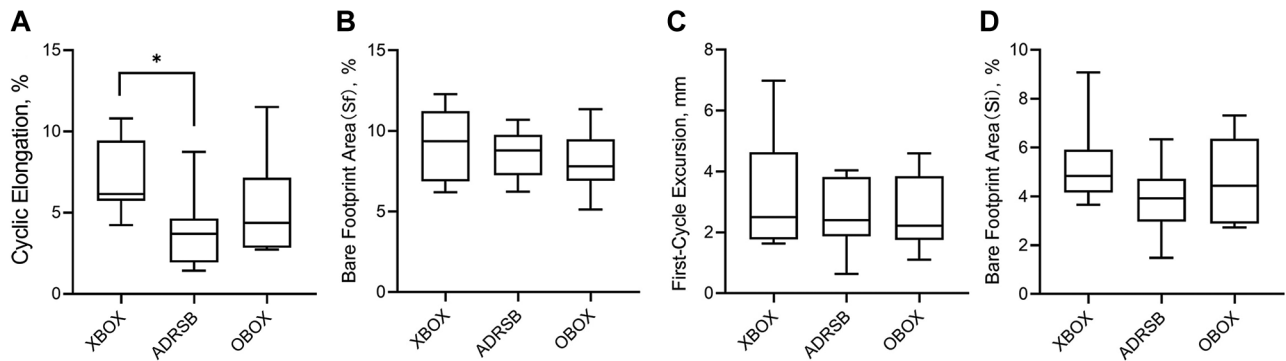[§]References: 3, 6, 8, 11, 14, 22, 24, 26, 27, 32, 33, 35, 36.

Figure 9. Boxplots presenting the mean (horizontal line), standard deviation (whiskers), and range (box) for (A) cyclic elongation, (B) the bare footprint area (Sf), BFA-Sf, (C) the first-cycle excursion, and (D) the bare footprint area (Si), BFA-Si. Significant differences between groups are indicated by $*P < .05$. BFA-Sf, footprint area at the end of the cycle; BFA-Si, ratio of the exposed area of the footprint area for the first cycle.

reported no significant differences in clinical outcomes between anchorless transosseous suture and anchored construct for rotator cuff tears.[8,32] Biomechanical experiments[2,4,5,10,13,16,17,29] have demonstrated that double-row anchors or transosseous-equivalent (TOE) repairs exhibit greater failure strength and smaller displacement gaps compared with single-row or transosseous suture. Nevertheless, these early findings were influenced by the lack of high-strength factors in the classic transosseous constructs, such as the number of sutures, suture limbs, and mattress stitches. According to a biomechanical review,[28] there is limited correlation between US and different constructs such as single-row, double-row, TOE, or transosseous suture. Instead, the US is associated with the suture material, the number of stitches, and mattress stitches.[9] Accordingly, we designed a novel high-strength transosseous suture configuration and termed it the OBOX. This construct increases the number of suture limbs, stitches, and mattress stitches, aiming to achieve higher US for transosseous suture.

The OBOX construct utilizes 6 sutures in 2 tunnels with 8 suture limbs, matching the number of suture limbs in the ADRSB construct with 2 medial-row anchors. Both the OBOX (2 tunnels) and ADRSB (2 anchors) have 8 stitches in the tendon, while the XBOX (2 tunnels) has 2 stitches in the tendon. Both the OBOX (2 tunnels) and ADRSB (2 anchors) have 4 narrow-range mattress stitches, while the XBOX (2 tunnels), which represents the highest strength of classic transosseous constructs, has only 1 wide-range mattress stitch.[28] The OBOX technique achieves narrow-range mattress stitches, with 2 suture limbs in 1 tunnel within the transosseous suture method. The sutures are reverse-pulled through the tunnel, and knots are tied by riding across the outer cortex of the humerus between the 2 tunnels. This action further draws the tendon into the bone tunnel, matching the concept of reducing sliding between the tendon and bone surfaces, as shown in Figure 10. Consequently, the OBOX exhibits theoretical strength superiority over classic transosseous constructs.

The XBOX construct was particularly prone to type 1 tears (6/8), whereas the OBOX construct was exclusively associated with type 2 tears (8/8). The ADRSB construct exhibited predominance of fixing material-related failure (6/8), followed by type 2 tears (2/8). In the ADRSB group, 6 cases had fixing material-related failure; the anchor was pulled off in 1 case, and sutures were broken at the anchor metal through-hole, with a cracking sound in the other 5 cases. The incidence of type 2 tendon tear was higher in the OBOX group than in the XBOX group. Type 2 re-tear has less remnant tendon than type 1 retear for revision. Both the OBOX (2 tunnels) and ADRSB (2 anchors) have 4 narrow-range mattress stitches, with 8 suture limb stitches in the medial row, while the XBOX (4 tunnels) has 1 wide-range mattress stitch with 2 suture limb stitches in the medial row. More suture limb stitches and narrow-range mattresses provide better tendon grip, but also increase the potential risk of type 2 retears. This may be a potential downside to the OBOX configuration. We suggest that the tendon should be repaired with high strength in a low-tension position to reduce inefficiency. The rate of type 2 retear should be controlled by selecting low-tension positions for repair, rather than by selecting low-strength constructs. Moreover, like the ADRSB construct, the OBOX construct can be partially or completely changed from narrow-range mattress stitches to knotless at the medial row based on the tendon quality and tension to reduce the probability of type 2 retear. Type 1 or type 2 tear is a factor we need to weigh, but it is not the unique criterion. In addition, in the OBOX configuration, although extra sutures may cause tendon "strangulation" and impede blood flow and healing, bone tunnels enrich the blood supply of the sutured rotator cuff underside. Ultrasonically, the transosseous suture provides better blood supply on both sides of the repaired rotator cuff than suture anchors.[34] With the progress of research, we have provided a novel high-strength transosseous construct whose strength is equivalent to that of the ADRSB. The OBOX construct has initially achieved a good balance in terms of fixation, durability, and cost-effectiveness. Although the cost of the OBOX
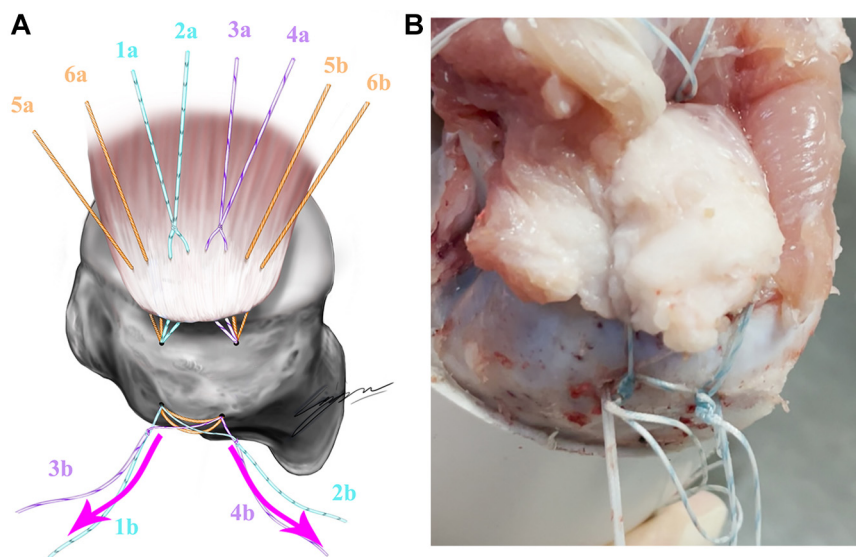
Figure 10. Reverse pulling of the sutures of the OBOX construct. (A) 1a and 2a, as well as 3a and 4a, were knotted to each other. The sutures were reverse-pulled through the tunnel, and knots were tied by riding across the outer cortex of the humerus between the 2 tunnels separately (3b and 1b; 4b and 2b). (B) Further drawing of the tendon into the bone tunnel.

construct is slightly higher than that of the XBOX, it is still much lower than that of the ADRSB construct. Because its strength is superior to that of traditional transosseous constructs, transosseous suture technology will not be abandoned in clinical practice because of concerns about its relatively low strength. This makes the OBOX construct a possible optional high-strength transosseous construct for rotator cuff repair.

Limitations

Several limitations should be acknowledged. Although good results have been obtained, there is still a bias regarding low fatigue resistance due to the noticeable lateral muscle migration on the bursal side of the porcine infraspinatus specimen. In addition, the lower elasticity of the muscle diminishes the wedge effect and self-reinforcement.[30] The infraspinatus tendons in the young pigs are stronger than elderly humans; thus, more force is required for sutures to pull through the tendons. Moreover, the bone density of specimens of 3-month-old pigs differs from that of humans. Consequently, experiments on human shoulder specimens are necessary to enhance the clinical applicability and reliability of the findings. The fatigue resistance test and failure test were conducted on the same specimen in this experiment, which may have led to structural relaxation before the failure test with lower US.

CONCLUSION

The OBOX construct exhibited a significantly higher mean US compared with the XBOX construct in a porcine

cadaveric model and was comparable with that of ADRSB repair. The most common modes of failure were type 2 tendon tear in the OBOX group, type 1 tendon tear in the XBOX group, and fixing material-related failure in the ADRSB group. The OBOX configuration represents a novel transosseous repair method with high fixation strength comparable with that of the ADRSB and stronger than that of the XBOX construct. However, caution must be exercised because of the potential for type 2 tendon tear associated with OBOX, which could complicate revision procedures. In the future, as it is further optimized and tested, the OBOX construct may be used as a high-strength transosseous construct that is equivalent to ADRSB for rotator cuff repair.

ORCID iDs

Zheng Yan (iD) https://orcid.org/0009-0001-9139-3457
Jia Ma (iD) https://orcid.org/0009-0003-8291-1210

REFERENCES

1. Abdelshahed M, Mahure SA, Kaplan DJ, et al. Arthroscopic rotator cuff repair: double-row transosseous equivalent suture bridge technique. *Arthrosc Tech*. 2016;5(6):e1297-e1304. PMID: 28149729
2. Ansah-Twum J, Belk JW, Cannizzaro CK, et al. Knotted transosseous-equivalent technique for rotator cuff repair shows superior biomechanical properties compared with a knotless technique: a systematic review and meta-analysis. *Arthroscopy*. 2022;38(3):1019-1027. PMID: 34606935
3. Arican M, Turhan Y, Karaduman ZO, Ayanoğlu T. Clinical and functional outcomes of a novel transosseous device to treat rotator cuff tears: a minimum 2-year follow-up. *J Orthop Surg (Hong Kong)*. 2019;27(3):2309499019875172. PMID: 31530075
4. Barber FA, Drew OR. A biomechanical comparison of tendon-bone interface motion and cyclic loading between single-row, triple-loaded

cuff repairs and double-row, suture-tape cuff repairs using biocomposite anchors. *Arthroscopy*. 2012;28(9):1197-1205. PMID: 22592123

5. Burkhart SS, Denard PJ, Obopilwe E, Mazzocca AD. Optimizing pressurized contact area in rotator cuff repair: the diamondback repair. *Arthroscopy*. 2012;28(2):188-195. PMID: 22035781

6. De Giorgi S, Ottaviani G, Bianchi FP, Delmedico M, Suma M, Moretti B. Single-row versus transosseous technique in the arthroscopic treatment of rotator cuff tears: a meta-analysis. *Eur J Orthop Surg Traumatol*. 2024;34(1):31-38. PMID: 37561195

7. Fama G, Tagliapietra J, Belluzzi E, Pozzuoli A, Biz C, Ruggieri P. Mid-term outcomes after arthroscopic ''tear completion repair'' of partial thickness rotator cuff tears. *Medicina (Kaunas)*. 2021;57(1):74. PMID: 33477332

8. Garofalo R, Calbi R, Castagna A, Cesari E, Budeyri A, Krishnan SG. Is there a difference in clinical outcomes and repair integrity between arthroscopic single-row versus transosseous (anchorless) fixation? A retrospective comparative study. *J Orthop Sci*. 2018;23(5):770-776. PMID: 30213364

9. Gülecyüz M, Bortolotti H, Pietschmann M, et al. Primary stability of rotator cuff repair: can more suture materials yield more strength? *Int Orthop*. 2016;40(5):989-997. PMID: 26442512

10. Hackl M, Nacov J, Kammerlohr S, et al. Intratendinous strain variations of the supraspinatus tendon depending on repair technique: a biomechanical analysis regarding the cause of medial cuff failure. *Am J Sports Med*. 2021;49(7):1847-1853. PMID: 33872064

11. Hinse S, Ménard J, Rouleau DM, Canet F, Beauchamp M. Biomechanical study comparing 3 fixation methods for rotator cuff massive tear: transosseous No. 2 suture, transosseous braided tape, and double-row. *J Orthop Sci*. 2016;21(6):732-738. PMID: 27633461

12. Kilcoyne KG, Guillaume SG, Hannan CV, Langdale ER, Belkoff SM, Srikumaran U. Anchored transosseous-equivalent versus anchorless transosseous rotator cuff repair: a biomechanical analysis in a cadaveric model. *Am J Sports Med*. 2017;45(10):2364-2371. PMID: 28520458

13. Kim DH, Elattrache NS, Tibone JE, et al. Biomechanical comparison of a single-row versus double-row suture anchor technique for rotator cuff repair. *Am J Sports Med*. 2006;34(3):407-414. PMID: 16282581

14. Liu XN, Yang CJ, Lee GW, Kim SH, Yoon YH, Noh KC. Functional and radiographic outcomes after arthroscopic transosseous suture repair of medium-sized rotator cuff tears. *Arthroscopy*. 2018;34(1):50-57. PMID: 29079262

15. Lorbach O, Bachelier F, Vees J, Kohn D, Pape D. Cyclic loading of rotator cuff reconstructions: single-row repair with modified suture configurations versus double-row repair. *Am J Sports Med*. 2008;36(8):1504-1510. PMID: 18296541

16. Ma CB, Comerford L, Wilson J, Puttlitz CM. Biomechanical evaluation of arthroscopic rotator cuff repairs: double-row compared with single-row fixation. *J Bone Joint Surg Am*. 2006;88(2):403-410. PMID: 16452754

17. Mazzocca AD, Millett PJ, Guanche CA, Santangelo SA, Arciero RA. Arthroscopic single-row versus double-row suture anchor rotator cuff repair. *Am J Sports Med*. 2005;33(12):1861-1868. PMID: 16210578

18. Park MC, ElAttrache NS, Tibone JE, Ahmad CS, Jun BJ, Lee TQ. Part I: footprint contact characteristics for a transosseous-equivalent rotator cuff repair technique compared with a double-row repair technique. *J Shoulder Elbow Surg*. 2007;16(4):461-468. PMID: 17321161

19. Pauly S, Kieser B, Schill A, Gerhardt C, Scheibel M. Biomechanical comparison of 4 double-row suture-bridging rotator cuff repair techniques using different medial-row configurations. *Arthroscopy*. 2010;26(10):1281-1288. PMID: 20887926

20. Plachel F, Traweger A, Vasvary I, Schanda JE, Resch H, Moroder P. Long-term results after arthroscopic transosseous rotator cuff repair. *J Shoulder Elbow Surg*. 2019;28(4):706-714. PMID: 30573430

21. Poppen NK, Walker PS. Forces at the glenohumeral joint in abduction. *Clin Orthop Relat Res*. 1978 Sep;(135):165-70. PMID: 709928.

22. Randelli P, Stoppani CA, Zaolino C, Menon A, Randelli F, Cabitza P. Advantages of arthroscopic rotator cuff repair with a transosseous suture technique: a prospective randomized controlled trial. *Am J Sports Med*. 2017;45(9):2000-2009. PMID: 28339286

23. Rossi LA, Rodeo SA, Chahla J, Ranalletta M. Current concepts in rotator cuff repair techniques: biomechanical, functional, and structural outcomes. *Orthop J Sports Med*. 2019;7(9):2325967119 868674. PMID: 31565664

24. Ryu RKN. Arthroscopic transosseous suture repair and single-row anchor fixation for rotator cuff lesions did not differ for pain, function, or rotator-cuff integrity at 15 months. *J Bone Joint Surg Am*. 2017;99(22):1943. PMID: 29135669

25. Salata MJ, Sherman SL, Lin EC, et al. Biomechanical evaluation of transosseous rotator cuff repair: do anchors matter? *Am J Sports Med*. 2013;41(2):283-290. PMID: 23239668

26. Sanders B. True transosseous hybrid rotator cuff repair. *Arthrosc Tech*. 2019;8(9):e1013-e1018. PMID: 31687334

27. Sandow MJ, Schutz CR. Arthroscopic rotator cuff repair using a transosseous knotless anchor (ATOK). *J Shoulder Elbow Surg*. 2020;29(3):527-533. PMID: 31563504

28. Shi BY, Diaz M, Binkley M, McFarland EG, Srikumaran U. Biomechanical strength of rotator cuff repairs: a systematic review and meta-regression analysis of cadaveric studies. *Am J Sports Med*. 2019;47(8):1984-1993. PMID: 29975549

29. Smith CD, Alexander S, Hill AM, et al. A biomechanical comparison of single and double-row fixation in arthroscopic rotator cuff repair. *J Bone Joint Surg Am*. 2006;88(11):2425-2431. PMID: 17079400

30. Smith GCS, Bouwmeester TM, Lam PH. Knotless double-row SutureBridge rotator cuff repairs have improved self-reinforcement compared with double-row SutureBridge repairs with tied medial knots: a biomechanical study using an ovine model. *J Shoulder Elbow Surg*. 2017;26(12):2206-2212. PMID: 28935379

31. Sobhy MH, Khater AH, Hassan MR, El Shazly O. Do functional outcomes and cuff integrity correlate after single- versus double-row rotator cuff repair? A systematic review and meta-analysis study. *Eur J Orthop Surg Traumatol*. 2018;28(4):593-605. PMID: 29442181

32. Srikumaran U, Huish EG, Jr, Shi BY, Hannan CV, Ali I, Kilcoyne KG. Anchorless arthroscopic transosseous and anchored arthroscopic transosseous equivalent rotator cuff repair show no differences in structural integrity or patient-reported outcomes in a matched cohort. *Clin Orthop Relat Res*. 2020;478(6):1295-1303. PMID: 32039957

33. Steinitz A, Buxbaumer P, Hackl M, Buess E. Arthroscopic transosseous anchorless rotator cuff repair using the X-box technique. *Arthrosc Tech*. 2019;8(2):e175-e181. PMID: 30906688

34. Urita A, Funakoshi T, Horie T, Nishida M, Iwasaki N. Difference in vascular patterns between transosseous-equivalent and transosseous rotator cuff repair. *J Shoulder Elbow Surg*. 2017;26(1):149-156. PMID: 27545051

35. Voigt C, Bosse C, Vosshenrich R, Schulz AP, Lill H. Arthroscopic supraspinatus tendon repair with suture-bridging technique: functional outcome and magnetic resonance imaging. *Am J Sports Med*. 2010;38(5):983-991. PMID: 20436053

36. Wang W, Kang H, Li H, Li J, Meng Y, Li P. Comparative efficacy of 5 suture configurations for arthroscopic rotator cuff tear repair: a network meta-analysis. *J Orthop Surg Res*. 2021;16(1):714. PMID: 34895286

37. Xu C, Zhao J, Li D. Meta-analysis comparing single-row and double-row repair techniques in the arthroscopic treatment of rotator cuff tears. *J Shoulder Elbow Surg*. 2014;23(2):18218-8. PMID: 24183478

38. Ying ZM, Lin T, Yan SG. Arthroscopic single-row versus double-row technique for repairing rotator cuff tears: a systematic review and meta-analysis. *Orthop Surg*. 2014;6(4):300-312. PMID: 25430714